

Thermal Stability Criteria of $\text{Se}_{80-x}\text{Te}_{20}\text{Sb}_x$ in Terms of Characteristic Temperatures and Kinetic Parameters

E.R. SHAABAN^{a,*}, H.A. ELSHAIKH^b AND M.M. SORAYA^b

^aPhysics Department, Faculty of Science, Al-Azhar University, Assuit, 71542, Egypt

^bDepartment of Physics, Faculty of Science, Aswan University, Egypt

(Received June 4, 2014; in final form March 29, 2015)

Thermal stability in terms of characteristic temperature and kinetic parameters of different compositions of glassy $\text{Se}_{80-x}\text{Te}_{20}\text{Sb}_x$ ($x = 0, 2, 4, 6, 8, 10$) have been investigated. Differential scanning calorimetry under non-isothermal conditions have been proposed to investigate thermal characteristic of these compositions. The thermal stability of these glasses was obtained in terms of various simple quantitative methods based on the characteristic temperatures, such as the glass transition temperature, T_g , the onset temperature of crystallization, T_{in} , the temperature corresponding to the maximum crystallization rate, T_p , and the melting temperature, T_m . Furthermore, the kinetic parameter $K_r(T)$ was achieved as another indicator for thermal stability and its results about stability compared with those evaluated by other criteria. The results of both the criteria and the kinetic parameter $K_r(T)$ confirm that the thermal stability increases with increase of Sb content. The results also refer to that: the glass transition T_g , activation energy of crystallization E_p and the frequency factor K_0 were increased with the addition of Sb. These results have been discussed in terms of the average coordination number, cohesive energy and average heat of atomization.

DOI: [10.12693/APhysPolA.128.358](https://doi.org/10.12693/APhysPolA.128.358)

PACS: 78.20.-e, 52.40.Db

1. Introduction

A great importance have been given to chalcogenide glasses due to their interesting and useful properties which made them one of the best candidates for many applications. Their applications as phase change memories (DVDs), X-ray medical image sensors, highly sensitive vidicons, holographic memories, nonlinear devices, solar cells, and ionic devices have been summarized by Tanaka and Shimakawa [1]. Se-Te alloys have much interest among chalcogenide glass materials because of their higher photosensitivity, greater hardness, higher crystallization temperature and smaller aging effects as compared to pure selenium [2–5]. The addition of third element to Se-Te alloys can improve their properties and make them more suitable for various applications. The insertion of Sb to the chalcogenide glasses expands the glass forming area and also creates compositional and configurational disorder in the system [6–8].

Furthermore, many interesting properties have been noted for Se-Te-Sb by the literatures [9–21], that lead to be Sb as a selective third element to the Se-Te binary system. Two different approaches have been adapted to investigate these materials, the first is the analysis of their structures and physical properties and the second is the study of glass transformation and crystallization process, i.e. thermal stability of chalcogenide glasses. Thermal stability has a great interest in technological applications, because the useful working temperature range will be determined by the structure changes and eventual

crystallization occurring at the operating temperatures, since the amorphous state is metastable one, it possesses the possibility of transformation into a more stable crystalline state.

Thermally activated transformations in the solid state can be investigated by isothermal and non-isothermal experiments [22–24]. In the isothermal method, the sample is brought quickly to a temperature above the temperature of glass transition (T_g) and the heat evolved during the crystallization process is recorded as a function of time. In the non-isothermal method, the sample is heated at a fixed rate and the heat evolved is again recorded as a function of temperature or time. A disadvantage of the isothermal technique is the impossibility of reaching a test temperature instantaneously and during the time in which the system needs to stabilize no measurements are possible. However, a constant heating rate experiment does not have this drawback [25].

Main goal of the present work is the investigation of the thermal stability and glass forming ability, for the $\text{Se}_{80-x}\text{Te}_{20}\text{Sb}_x$ ($x = 0, 2, 4, 6, 8, 10$) chalcogenide glass system. The results have been obtained under non-isothermal conditions using differential scanning calorimetry (DSC). The effect of Sb additive on glass transition T_g , activation energy of glass transition E_g and activation energy of crystallization E_p have been discussed in terms of the average coordination number, cohesive energy and average heat of atomization.

2. Theoretical basis

2.1. Thermal stability parameters in terms of characteristic temperature

In accordance with the characteristic temperatures such as the glass transition temperature, T_g , the onset

*corresponding author; e-mail: esam_ramadan2008@yahoo.com

temperature of crystallization, T_{in} , the temperature corresponding to the maximum crystallization rate, T_p , and the melting temperature, T_m , many stability criteria have been proposed. Using the ratio, proposed by Kauzmann for typical single component glass T_g/T_m [26], the first thorough study on the glass thermal stability of various compounds was done by Sakka and Mackenzie [27]. Dietzel introduced the glass criterion [28]:

$$\Delta T = T_{in} - T_g, \quad (1)$$

which is often an important parameter to evaluate the thermal stability of the glasses. The H_r criterion developed by Hruby [29]:

$$H_r = \Delta T / (T_m - T_p) \quad (2)$$

and compositional dependences of the Hruby coefficient were survived by Šesták [30]. On the basis of the H_r criterion, Saad and Poulain [31] obtained two other criteria, weighted thermal stability, H' and S criterion,

$$H' = \Delta T / T_g \text{ and } S = (T_p - T_{in}) \Delta T / T_g. \quad (3)$$

The glass forming tendency K_{gl} is given by

$$K_{gl} = \frac{(T_{in} - T_g)}{(T_m - T_g)} \quad (4)$$

and it is more suitable than ΔT for estimating the glass thermal stability.

2.2. Thermal stability in terms of kinetic parameters

On the other side, on the basis of the formal theory of transformation kinetics, the evolution with time, t , of the volume fraction crystallized, x , in terms of the crystal growth rate, u defined as [32]:

$$\chi = 1 - \exp \left(-g \left(\int_0^t u(t') dt' \right)^n \right) = 1 - \exp(-I_1^n). \quad (5)$$

Here, g is a geometric factor and n — an exponent, which depends on the mechanism of transformation. Differentiating Eq. (5) with respect to time and taking into account the Arrhenius temperature dependence for the crystal growth, crystallization rate is obtained as

$$\frac{d\chi}{dt} = n(1 - \chi) I_1^{n-1} K_0 \exp \left(\frac{-E_c}{RT} \right) = nK(1 - \chi) I_1^{n-1}, \quad (6)$$

where E_c is the effective activation energy for crystal growth and K is the reaction rate constant, which has an Arrhenius temperature dependence according to the relation

$$K(T) = K_0 \exp \left(-\frac{E_c}{RT} \right). \quad (7)$$

Surinach et al. [33] introduced $K(T_g)$ criterion and Hu and Jiang [34] developed the $K(T_p)$ criterion

$$K(T_g) = K_0 \exp \left(-\frac{E_c}{RT_g} \right) \quad (8a)$$

and

$$K(T_p) = K_0 \exp \left(-\frac{E_c}{RT_p} \right). \quad (8b)$$

Thus, the values of these two parameters indicate the tendency of glass to devitrify on heating. The larger their values the greater is the tendency to devitrify. It is reasonable to assess the glass stability by a kinetic parameter, $K(T)$ whereas the formation of glass is a kinetic process. The H_r parameter itself is a stability factor based on characteristic temperatures. Here a stability criterion is defined as:

$$K_r(T) = K_0 \exp \left(-\frac{H_r E_c}{RT} \right), \quad (9)$$

where T is any temperature between T_g and T_p . The theoretical background for the definition of the parameter $K_r(T)$ based on the analysis of the relation between the parameters $K(T)$ and $K_r(T)$. Differentiating the expressions of both parameters results in

$$dK_r = H_r E K_r (RT^2)^{-1} dT, \quad dK = E K (RT^2)^{-1} dT$$

and the relative variation in each parameter per kelvin is

$$\frac{\Delta K_r}{K_r \Delta T} = \frac{H_r E}{RT^2}, \quad \frac{\Delta K}{K \Delta T} = \frac{E}{RT^2}.$$

It should be noted that the above-mentioned variation of the parameter $K_r(T)$ is H_r times the variation in parameter $K(T)$, which could justify the accuracy of the parameter $K_r(T)$. Just like the $K(T)$ criteria, the smaller the values of $K_r(T)$, the greater is the thermal stability of the glass. The obvious advantage of this method is that it can evaluate the glass stability over a broad temperature range other than at only one temperature such as T_g or T_p .

3. Experimental details

Different compositions of $Se_{80-x}Te_{20}Sb_x$ ($x = 0, 2, 4, 6, 8, 10$) bulk chalcogenide samples were prepared according to the conventional melt-quenched technique. The Se, Te, and Sb elements of high-purity (5N, Aldrich and Sigma chemical company) were weighted according to their atomic percentage and placed together in a precleaned and outgassed silica ampoule, which was evacuated to a pressure of about 10^{-4} Pa and then sealed. The synthesis was performed in a programmable rocking furnace and slowly heated up to approximately 950°C with the temperature ramp about $5^\circ\text{C}/\text{min}$, for about 24 h. During the melt process, the ampoule was inverted at regular time intervals (≈ 1 h) so that the amorphous solid will be homogeneous and isotropic. After the synthesis, the melt was quenched rapidly in ice water to obtain the Se-Te-Sb glassy alloy. Then the solid was broken along its natural stress line into smaller pieces suitable for grinding. Both the homogeneity and the compositional contents of the prepared samples were checked using energy-dispersive analysis of X-rays (EDAX). It was found that the percentage ratios of the constituent elements were close to

the values taken for the starting alloys. The glassy nature of the materials was confirmed via X-ray scanning in a Philips diffractometer 1710, using Cu as target and Ni as filter ($\lambda = 1.5418 \text{ \AA}$). These showed an absence of peaks characteristic of crystalline phases. The calorimetric measurements were carried out in a differential scanning calorimeter Shimadzu 50 with an accuracy of $\pm 0.1 \text{ K}$. The calorimeter was calibrated, for each heating rate, using well-known melting temperatures and melting enthalpies of zinc and indium supplied with the instrument. Twenty mg powdered samples, crimped into aluminium pans, were scanned at different heating rates ($\beta = 5, 10, 20, 30, 40 \text{ K/min}$). The temperatures of the glass transition, T_g , the crystallization extrapolated onset, T_{in} , the crystallization peak, T_p and the melting temperature T_m were determined with an accuracy of $\pm 1 \text{ K}$.

4. Results and discussion

In order to investigate the thermal properties of $\text{Se}_{80-x}\text{Te}_{20}\text{Sb}_x$ ($x = 0, 2, 4, 6, 8, 10$) chalcogenide glasses, DSC experiments were carried out at different heating rates in the range 5–40 K/min. Figure 1a shows the

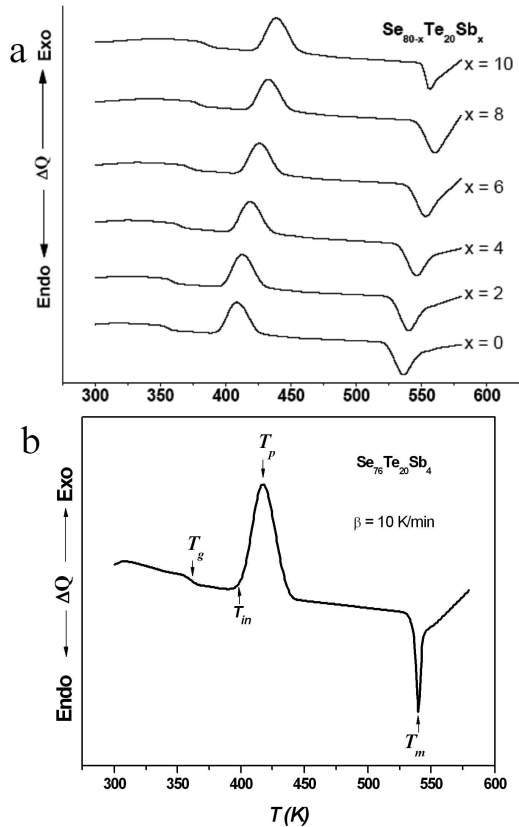


Fig. 1. The DSC traces of the as prepared $\text{Se}_{80-x}\text{Te}_{20}\text{Sb}_x$ ($x = 0, 2, 4, 6, 8, 10$) compositions at heating rate $\beta = 10 \text{ K/min}$. (b) The DSC curvature of the as prepared $\text{Se}_{76}\text{Te}_{20}\text{Sb}_4$ composition at heating rate $\beta = 10 \text{ K/min}$ (demonstrating the four characteristic temperatures as referred by arrows).

TABLE I

The values of thermal parameters of glass transition temperature T_g , onset temperature of crystallization T_{in} , crystallization temperature T_p and melting temperature T_m of $\text{Se}_{80-x}\text{Te}_{20}\text{Sb}_x$ ($0 \leq x \leq 10$) alloys with different heating rates β . The characteristic parameters K_{gl} , H_r and S according to the text.

β	T_g [K]	T_{in} [K]	T_p [K]	T_m [K]	K_{gl}	H_r	H'	S [K]
$x = 0$								
5	345	380	397	526	0.1934	0.2713	0.1014	1.7246
10	355	390	407	536				
20	366	401	418	547				
30	373	408	425	554				
40	377	412	429	558				
$x = 2$								
5	347	385	401	529	0.2088	0.2969	0.1095	1.7522
10	357	395	411	539				
20	368	406	422	550				
30	375	413	429	557				
40	379	417	433	561				
$x = 4$								
5	351	391	407	531	0.2222	0.3226	0.114	1.8234
10	361	401	417	541				
20	372	412	428	552				
30	379	419	435	559				
40	383	423	439	563				
$x = 6$								
5	355	398	415	536	0.2376	0.3554	0.1211	2.0592
10	365	408	425	546				
20	376	419	436	557				
30	383	426	443	564				
40	387	430	447	568				
$x = 8$								
5	359	405	422	540	0.2541	0.3898	0.1281	2.1783
10	369	415	432	550				
20	380	426	443	561				
30	387	433	450	568				
40	391	437	454	572				
$x = 10$								
5	362	411	428	545	0.2678	0.4188	0.1354	2.3011
10	372	421	438	555				
20	383	432	449	566				
30	390	439	456	573				
40	394	443	460	577				

DSC traces of the as prepared $\text{Se}_{80-x}\text{Te}_{20}\text{Sb}_x$ compositions at heating rate $\beta = 10 \text{ K/min}$. It is easily seen four characteristic phenomena in the studied temperature region. As shown by Fig. 1b for $\text{Se}_{76}\text{Te}_{20}\text{Sb}_4$ sample: the first is the glass transition temperature, the second is the initial temperature of crystallization, the third is the crystallization temperature and the last is the melting temperature. Numerical values of these characteristic temperatures are given in Table I. The variation of T_g with various compositions of $\text{Se}_{80-x}\text{Te}_{20}\text{Sb}_x$ is shown ob-

viously in Table I. It is observed that there is an increase in T_g with increasing Sb content. On the other side, the average coordination number, Z , of $Se_xTe_ySb_z$ ternary compound ($x + y + z = 1$) can be expressed as [35]:

$$Z = (x\text{CN}(\text{Se}) + y\text{CN}(\text{Te}) + z\text{CN}(\text{Sb})). \quad (10)$$

The calculated values of Z of $Se_{80-x}Te_{20}Sb_x$ ($x = 0, 2, 4, 6, 10$) films are listed in Table II. It can be seen that coordination number increases with increase of the Sb content (as a result of Sb additive to Se-Te matrix). This increase of Z may probably result in increase of T_g with further increase of Sb. In general, the T_g of multicomponent glass is known to depend on many interdependent parameters such as band gap, bond energy, effective molecular weight, the type and fraction of various structural units formed, cohesive energy, the average heats of atomization and the average coordination number [36–38]. Furthermore, the number of lone pairs that characterize the flexibility of the compositions, also related to a variation of T_g . The number of lone pairs associated with the compositions under investigation was calculated according to the relation [39]:

$$L = V - Z, \quad (11)$$

where L and V are lone-pair electrons and valence electron, respectively. The calculated values of lone pair electrons are given in Table II. It is obvious that the number of lone pairs electrons decreases with increasing Sb content within the composition and this enhances with evidence the increase of T_g with increasing Sb content, since decreasing number of lone pair electrons increases the strain energy i.e. increases the rigidity of the system, hence the glass transition increases, so the larger number of lone pair electrons in the structure favour stable glass formation [39]. Also it is clear from Table I, that T_g increases gradually with increasing the heating rate for each specimen. An empirical relationship has been suggested by Lasocka [40] to describe the dependence of the temperature of the glass transition on the heating rate and has the form

$$T_g = A + B \ln \beta, \quad (12)$$

where A and B are constants for a given glass compositions. Plots of T_g versus $\ln \beta$ for the $Se_{80-x}Te_{20}Sb_x$ glasses are shown in Fig. 2. The calculated values of A and B are listed in Table III. It was previously suggested that the value of B depends on the glass composition and the quenching rate from the melt. The same cooling rate was used for preparing the different compositions of the present work. Increasing the Sb content results in the increase of constant B .

4.1. Evaluation of activation energies for glass transition E_g and for crystallization E_c

The activation energy of glass transition was determined using the values of T_{ag} according to their corresponding heating rates across the Kissinger relation, which was basically derived for the crystallization process and suggested to be valid for the glass transition [41]. This relation is given by

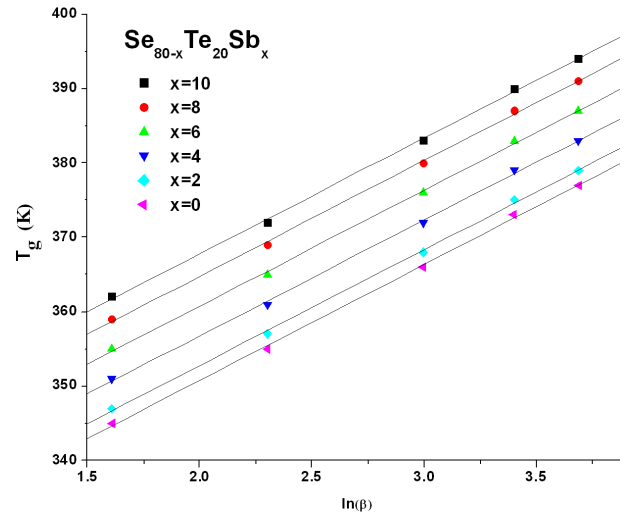


Fig. 2. Plots of T_g versus $\ln \beta$ for the $Se_{80-x}Te_{20}Sb_x$ ($x = 0, 2, 4, 6, 8, 10$) glasses.

TABLE II

Physical parameters of the constituent elements.

Property	Se	Te	Sb
energy gap [eV]	1.95	0.65	0.15
density [g/cc]	4.79	6.24	6.62
coordination number	2	2	3
atomic radius [Å]	1.22	1.42	1.53
electronegativity	2.55	2.1	2.05
bond energy [kcal mol ⁻¹]	44.04	33	30.22
heat of atomization [Kcal mol ⁻¹]	49.4	46	62

TABLE III

The average coordination number Z , the average heat of atomization H_s , the cohesive energy CE, numbers of lone pairs electrons L and A, B constants as a function of Sb content of the $Se_{80-x}Te_{20}Sb_x$ glassy compositions.

Sb [at.%]	L	A	B	Z	CE [eV]	H_s [kcal/g/atom]
0	4	16.1	319	2	1.912	48.72
2	3.96	15.5	321	2.02	1.931	48.972
4	3.92	16.2	325	2.04	1.95	49.224
6	3.88	15.7	329	2.06	1.969	49.476
8	3.84	16.2	333	2.08	1.988	49.728
10	3.8	15.6	336	2.1	2.007	49.98

$$\ln \left(\frac{T_g^2}{\beta} \right) = \frac{E_g}{RT_g} + \text{const}, \quad (13)$$

where R is the universal gas constant. Figure 3 shows the relation between $\ln \left(\frac{T_g^2}{\beta} \right)$ versus $(1/T_g)$, the values of E_g obtained from the slope of the straight line corresponding to each specimen. These values (not shown

TABLE IV

Kinetics parameters $K(T)$ and $K_r(T)$ for the $\text{Se}_{80-x}\text{Te}_{20}\text{Sb}_x$ ($0 \leq x \leq 10$) alloys.

Alloy β	$K(T_g)$ [s ⁻¹]	$K(T_p)$ [s ⁻¹]	$K_r(T_g)$ [s ⁻¹]	$K_r(T_p)$ [s ⁻¹]
$x = 0$				
5	0.00012	0.00537	216180	612315
10	0.00026	0.01004	270431	725575
20	0.00062	0.0193	341102	866339
30	0.00104	0.02874	392601	965196
40	0.00139	0.03588	424452	1025050
$x = 2$				
5	9.82×10^{-5}	0.00537	116712	382913
10	0.00023	0.01004	149433	461078
20	0.00054	0.01932	193095	559885
30	0.0009	0.02878	225535	630244
40	0.00121	0.03594	245829	673192
$x = 4$				
5	8.35×10^{-5}	0.00537	67035	256886
10	0.00019	0.01005	87854	314365
20	0.00046	0.01934	116326	388299
30	0.00078	0.02884	137903	441698
40	0.00105	0.03603	151561	474570
$x = 6$				
5	5.98×10^{-5}	0.00538	30759	152160
10	0.00014	0.01006	41643	190091
20	0.00034	0.01937	57042	239976
30	0.00058	0.02891	69034	276665
40	0.00078	0.03614	76749	299496
$x = 8$				
5	4.65×10^{-5}	0.00538	12567	80068
10	0.00011	0.01006	17589	102221
20	0.00027	0.0194	24943	132038
30	0.00046	0.02898	30832	154385
40	0.00063	0.03624	34684	168449
$x = 10$				
5	2.52×10^{-5}	0.00376	3931	31984
10	6.03×10^{-5}	0.00704	5665	41585
20	0.00015	0.01358	8284	54762
30	0.00026	0.02029	10432	64796
40	0.00035	0.02539	11858	71171

in tables) give increasing trend of E_g with increase of Sb contents. The increase of E_g results in the increase of T_g .

For the evaluation of the activation energy of crystallization E_c using the variation of T_p with β according to the Kissinger relation [41] which is modified by Vazquez et al. [42] for non-isothermal analysis as follows:

$$\ln\left(\frac{T_p^2}{\beta}\right) = \frac{E_c}{RT_p} + \ln\left(\frac{E_c}{RK_0}\right). \quad (14)$$

From the experimental data, a plot of $\ln\left(\frac{T_p^2}{\beta}\right)$ versus $1/T_p$ has been drawn for different compositions showing the straight regression line in Fig. 4. The activation

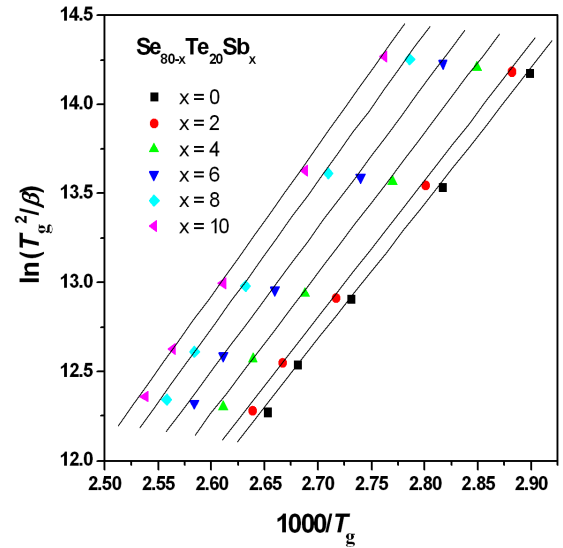


Fig. 3. Plots of $\ln\left(\frac{T_g^2}{\beta}\right)$ versus $(1/T_g)$ of $\text{Se}_{80-x}\text{Te}_{20}\text{Sb}_x$ ($x = 0, 2, 4, 6, 8, 10$) glassy alloys and straight regression lines for all these alloys.

energy, E_c and the frequency factor, K_0 are then evaluated by least squares fitting method of Eq. (14). Figure 5 shows the values of E_c and K_0 as a function of Sb content. The frequency factor, K_0 (which measures the probability of effective molecular collisions for the formation of the activated complexes in each case), increases with increasing Sb content. It is observed that E_c increase with increasing antimony content within the composition. The trend of the activation energy can be interpreted in term of the bond energies.

In view of the chemical bond approach to examine the structure and properties of various types of chalcogenide glasses, atoms combine more favorably with atoms of different kinds than with the same kind; this assumption which is generally found to be valid for glass structures, has been used by Zachariassen [43] in his covalently bonded continuous random net work model. On using this assumption, bonds between like atoms will only occur if there is an excess of a certain type of atoms. Bonds are formed in the sequence of decrease of bond energies until all available valences for the atoms are saturated. The bond energies $D(A-B)$ for heteronuclear bonds have been calculated by using the relation [44]:

$$D(A-B) = [D(A-A) \times D(B-B)]^{1/2} + 30(\chi_A - \chi_B)^2, \quad (15)$$

where $D(A-A)$ and $D(B-B)$ are the energies of the homonuclear bonds, χ_A and χ_B are electronegativity values for atoms involved. Both the electronegativity and the homonuclear bonds $D(A-A)$ and $D(B-B)$ for Te, Se, and Sb are listed in Table II.

The types of bonds expected to occur in the system under investigation are Se-Te bonds (44.2 kcal/mol), Se-

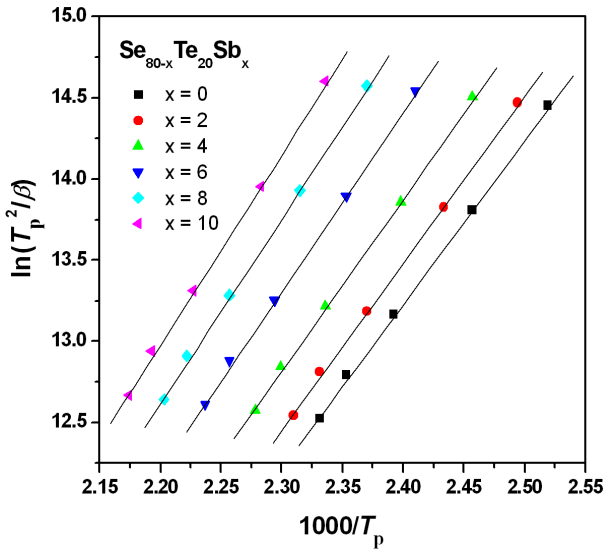


Fig. 4. Plots of $\ln\left(\frac{T_p^2}{\beta}\right)$ versus $(1/T_p)$ of $Se_{80-x}Te_{20}Sb_x$ ($x = 0, 2, 4, 6, 8, 10$) glassy alloys and straight regression lines for all these alloys.

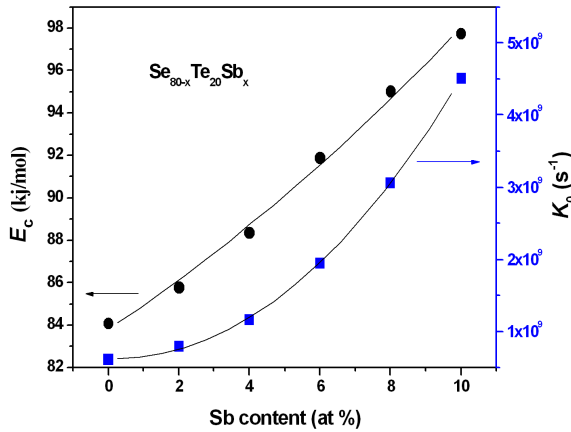


Fig. 5. The values of the activation energies E_c and the frequency factors K_0 as a function of Sb content.

Sb (43.98 kcal/mol) and Se–Se (44.04 kcal/mol). In the present compositions the Se atoms strongly bond to Te. The Se–Te bonds have the highest probability to form, then the Se–Sb bonds. After these bonds are formed, there are still unsatisfied Se valences, which are much satisfied by the formation of Se–Se bond. The number of excess Se–Se homopolar bonds for each composition of the $Se_{80-x}Te_{20}Sb_x$ ($x = 0, 2, 4, 6, 10$) are listed in Table II. Knowing the bond energies, the cohesive energy (CE) have been derived by assuming the bond energies over all the bonds expected in the system under test by the following equation:

$$CE = \sum C_i D_i / 100, \quad (16)$$

where C_i and D_i are the numbers of expected chemical bonds and the energy of each corresponding bond. The results of CE are listed in Table III. It should be mentioned that the approach of the chemical bond ne-

glects dangling bond and other valence defects as a first approximation. Also van der Waals interactions are neglected, which can provide a means for further stabilization by the formation of much weaker links than regular covalent bonds.

In order to complete the vision of the chemical bonds, it is appropriate to obtain the average heat of atomization H_s , which is defined as a direct measure of cohesive energy and considered as the average bond strength. For a compound $A_x B_y C_z$ it can be calculated, in kcal/g/atom, as the formula [45]:

$$H_s = \frac{\alpha H_s^A + \beta H_s^B + \gamma H_s^C}{x + y + z}, \quad (17)$$

where H_s^A , H_s^B , H_s^C is the heat of atomization of the involved elements (Se, Te, Sb) as shows Table II and x, y, z are the ratios of these elements in the chalcogenide glass system, respectively. The values of H_s for the Se–Te–Sb glass are shown in Table II. These results may be due to that the decrease of the relative atomic mass of chalcogen (Se) or its proportion in a given chalcogenide glass system, increases the average bond strength [46, 47]. These obtained results of cohesive energy and the average heat of atomization reflect the reason behind the increase of activation energy of glass transition, glass transition and activation energy of crystallization with increase of antimony content within the composition.

4.2. Thermal stability and the ability of glass formation

The thermal stability criteria and the glass forming tendency using the characteristic temperatures T_g , T_{in} , T_p , and T_m are given in Table I. It is clear that the glass forming tendency k_{gl} as calculated according to Eq. (4) being constant with the variation of the heating rate for each specimen, but it vary obviously with varying the Sb content within the composition, i.e. the glass forming tendency k_{gl} increases with increase of antimony content.

Also as shown in Table I, H_r is constant with increase of heating rate for each sample, but it increases more and more with further addition of antimony into the composition. It is also observed as given in Table I that H' and $S(k)$ criteria decrease with increase of heating rate for all the samples but they increases with increase of Sb content within the composition. From the above mentioned results, it is easily seen that the glass forming ability and the glass thermal stability increase with the addition of antimony to the Se–Te binary system. After knowing the values of E and K_0 as mentioned above, parameters $K(T)$ and $K_r(T)$ of studied alloys were calculated by using the relationships: Eqs. (7) and (9), respectively. These calculations were carried out in order to compare the stability sequence of the studied materials from the quoted parameters with the corresponding sequence deduced from stability criteria based on characteristic temperatures.

Figures 6 and 7 represent the plots of $K_r(T)$ versus T at two different heating rates $\beta = 30$ K/min and $\beta = 10$ K/min, respectively. It was clear according to the

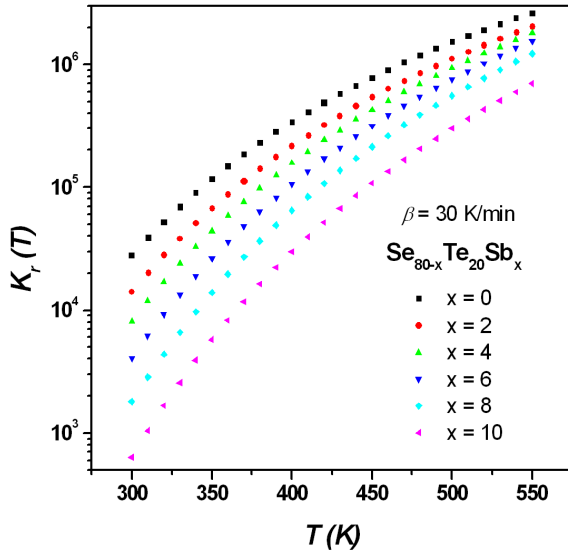


Fig. 6. Plots of $K_r(T)$ versus T of $\text{Se}_{80-x}\text{Te}_{20}\text{Sb}_x$ ($x = 0, 2, 4, 6, 8, 10$) glassy alloys at $\beta = 30$ K/min.

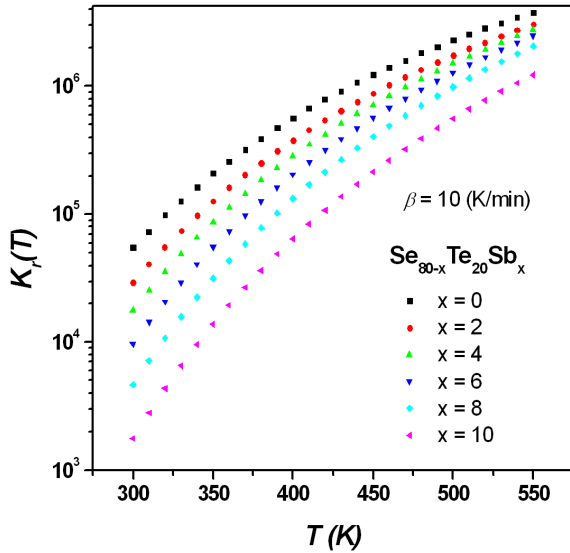


Fig. 7. Plots of $K_r(T)$ versus T of $\text{Se}_{80-x}\text{Te}_{20}\text{Sb}_x$ ($x = 0, 2, 4, 6, 8, 10$) glassy alloys at $\beta = 10$ K/min.

last two figures that $K_r(T)$ decreases with increase of Sb content over the entire temperature range, that means a higher stability for the compositions containing larger amounts of Sb. Hence this result emphasizes the last result of thermal stability obtained by H , H_r and S criteria related to characteristic temperatures T_g , T_{in} , T_p , T_p (shown by Table I). It is found that $K_r(T)$ of all the samples increases rapidly over the temperature 300–370 K, then it increases quite slowly over the temperature range 380–450 K and then much slowly in the range 460–550, that means the thermal stability decreases rapidly in the range of glass transition, quite slowly in the range of initial and crystallization temperatures, then it decreases much slowly reaching to the melting temperature, since

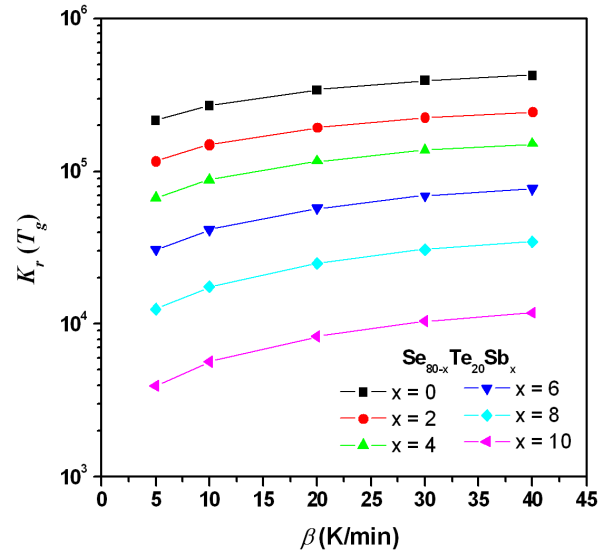


Fig. 8. The variation of $K_r(T_g)$ with heating rates for $\text{Se}_{80-x}\text{Te}_{20}\text{Sb}_x$ ($x = 0, 2, 4, 6, 8, 10$) glassy compositions.

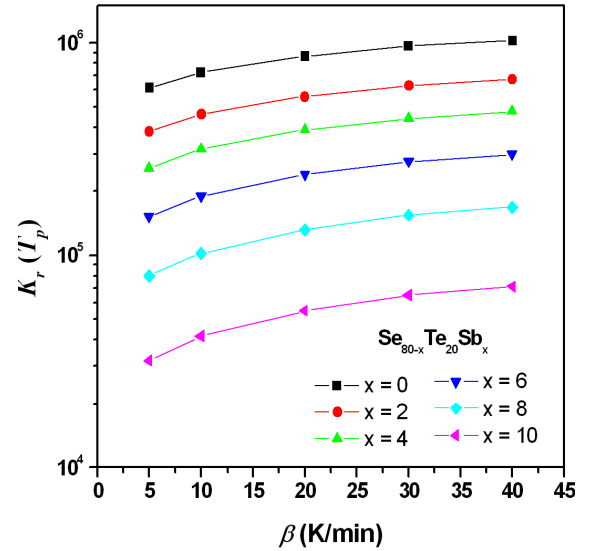


Fig. 9. The variation of $K_r(T_p)$ with heating rates for $\text{Se}_{80-x}\text{Te}_{20}\text{Sb}_x$ ($x = 0, 2, 4, 6, 8, 10$) glassy compositions.

the glassy state is a metastable state, i.e. the thermal stability varies more rapidly in this region.

The values of $K(T)$ and $K_r(T)$ for the temperatures T_g and T_p are listed in Table IV. The values of $K_r(T_g)$ and $K_r(T_p)$ are deduced using the relation given by Eq. (9). Figures 8, 9 represent the variation of $K_r(T_g)$ and $K_r(T_p)$ with heating rates for all the alloys under investigation, respectively. It is clear that $K_r(T_g)$ increases with increase of heating rates for all the alloys and it decreases with increase of Sb content within the specimen, i.e. thermal stability increases with increase of Sb content and decreases with increase of heating rates for all compounds under study. The $K_r(T_p)$ follows the same man-

ner of $K_r(T_g)$ emphasizing the same results of glass stability associated with these compositions. In a good agreement of our results, Shaaban et al. [14] and Prashanth and Asokan [13] have found that the addition of Sb to the Se–Te binary system enhance the glass thermal stability and glass forming tendency. Also across an investigation for $Se_{80-x}Te_{20}Sb_x$ ($x = 1.5, 7.5, 9$). Moharram et al. [48] have found that the compositions of larger amounts of Sb have a higher stability. The deduced values of $K(T_g)$ and $K(T_p)$ criteria were calculated using the above mentioned relations given by Eqs. (8a, 8b), respectively. Their values are listed in Table IV. It was observed that $K(T_g)$ have a slight increase with increase of heating rate for all the compositions but it decreases slightly with increase of Sb content, that means a higher resistance to devitrify with increase of Sb content and a higher tendency to devitrify with increase of heating rate for all the specimens. On the other hand, $K(T_p)$ as shown in Table IV gives a slight increase with increase of the heating rate and almost unnoticeable increase with increase of Sb content, that is probably indicates to a higher tendency to devitrify with Sb addition at the crystallization temperature T_p , which is strongly correlated with this criterion ($K(T_p)$).

5. Conclusion

A calorimetric study under non-isothermal conditions has been introduced to research of the thermal characteristic of the $Se_{80-x}Te_{20}Sb_x$ ($x = 0, 2, 4, 6, 8, 10$) glassy compositions. The thermal properties results obtained by various criteria as H_r , H' , S and k_{gl} that based on characteristic temperatures T_g , T_{in} , T_p , T_m (as mentioned in text) indicate to that the compositions with higher amounts of Sb have a higher thermal stability and a higher glass forming tendency. The K_r criterion which correlated with the activation energy of crystallization has emphasized the same results of stability of these glasses. The results also refer to that: the glass transition T_g , activation energy of crystallization E_p and the frequency factor K_0 were increased with the addition of Sb, these results have been discussed in terms of the average coordination number, cohesive energy, and average heat of atomization.

Acknowledgments

The authors are grateful to Al Azhar University — Faculty of Science, Physics Department, Assuit branch, for financial support. Aswan university Faculty of Science — Physics Department is also acknowledged.

References

- [1] K. Tanaka, K. Shimakawa, *Amorphous Chalcogenide Semiconductors and Related Materials*, Springer Sci. + Business Media, Berlin 2011.
- [2] E.R. Shaaban, M.T. Dessouky, A.M. Abousehly, *Philos. Mag.* **88**, 1099 (2008).
- [3] A. Arora, A. Goel, E.R. Shaaban, O.P. Pandey, J.M.F. Ferreira, *Physica B* **403**, 1738 (2008).
- [4] N. Sharma, S. Kumar, *Turk. J. Phys.* **31**, 161 (2007).
- [5] A. Bhargava, A. Williamson, Y.K. Vijay, I.P. Jain, *J. Non-Cryst. Solids* **192–193**, 494 (1995).
- [6] A. Dahshan, *J. Non-Cryst. Solids* **354**, 3034 (2008).
- [7] J.L. Cadenas-Leal, J. Vazquez, D.G. Barreda, P.L. Lopez-Aleman, P. Villares, R. Jiménez-Garay, *Thermochim. Acta* **484**, 70 (2009).
- [8] A.H. Moharram, A.A. Othman, H.H. Amer, A. Dahshan, *J. Non-Cryst. Solids* **352**, 2187 (2006).
- [9] D.K. Dwivedi, H.P. Pathak, R.K. Shukla, A. Kumar, *Am. J. Mater. Sci. Eng.* **1**, 46 (2013).
- [10] M.K. Vanitha, M.V. Hanumantha Rao, S. Asokan, K. Ramesh, *J. Phys. Chem. Solids* **74**, 804 (2013).
- [11] M. Fadel, N.A. Hegab, I.S. Yahia, A.M. Salem, A.S. Farid, *J. Alloys Comp.* **509**, 7663 (2011).
- [12] A. Arora, E.R. Shaaban, K. Singh, O.P. Pandey, *J. Non-Cryst. Solids* **354**, 3944 (2008).
- [13] S.B. Bhanu Prashanth, S. Asokan, *J. Non-Cryst. Solids* **355**, 164 (2009).
- [14] E.R. Shaaban, Ishu Kansal, M. Shapaan, J.M.F. Ferreira, *J. Thermal Anal.* **98**, 347 (2009).
- [15] A. Goel, D.U. Tulyaganov, M.J. Pascual, E.R. Shaaban, F. Munoz, Z. Lü, J.M.F. Ferreira, *J. Non-Cryst. Solids* **356**, 1070 (2010).
- [16] A.S. Soltan, *Appl. Phys. A* **80**, 117 (2005).
- [17] E.R. Shaaban, M.Y. Hassaan, A.G. Mostafa, A.M. Abdel-Ghany, *J. Alloys Comp.* **482**, 440 (2009).
- [18] S.K. Tripathi, V. Sharma, A. Thakur, J. Sharma, G.S.S. Saini, N. Goyal, *J. Non-Cryst. Solids* **351**, 2468 (2005).
- [19] E.R. Shaaban, H.A. Elshaikh, M.M. Soraya, *Int. J. New. Hor. Phys.* **1**, 9 (2014).
- [20] N.S. Saxena, *J. Non-Cryst. Solids* **345**, 161 (2004).
- [21] E.R. Shaaban, S.H. Mohamed, *J. Thermal Anal.* **107**, 617 (2012).
- [22] N. Rysava, T. Spasov, L. Tichy, *J. Thermal Anal.* **32**, 1015 (1987).
- [23] A. Giridhar, S. Mahadevan, *J. Non-Cryst. Solids* **51**, 305 (1982).
- [24] E.R. Shaaban, M.T. Dessouky, A.M. Abousehly, *J. Phys. Condens. Matter* **19**, 11 (2007).
- [25] M.J. Strink, A.M. Zahra, *Thermochim. Acta* **298**, 179 (1997).
- [26] W. Kauzmann, *Chem. Rev.* **43**, 219 (1948).
- [27] S. Sakka, J.D. Mackenzie, *J. Non-Cryst. Solids* **6**, 145 (1971).
- [28] A. Dietzel, *Glasstech* **22**, 41 (1968).
- [29] A. Hruby, *Czech J. Phys. B* **22**, 1187 (1972).
- [30] J. Šesták, *J. Therm. Anal.* **33**, 75 (1988).
- [31] M. Saad, M. Poulain, *Mater. Sci. Forum* **19**, 11 (1987).
- [32] H. Yinnon, D.R. Uhlmann, *J. Non-Cryst. Solids* **54**, 253 (1983).
- [33] S. Surinach, M.D. Baro, M.T. Clavaguera-Mora, N. Clavaguera, *J. Mater. Sci.* **19**, 3005 (1984).

- [34] L. Hu, Z. Jiang, *J. Chin. Ceram. Soc.* **18**, 315 (1990).
- [35] E.R. Shaaban, I.S. Yahia, M. Fadel, *J. Alloys Comp.* **469**, 427 (2009).
- [36] A. Gridhar, S. Mahadevan, *J. Non-Cryst. Solids* **151**, 245 (1992).
- [37] A.F. Ioffe, A.R. Regel, *Prog. Semicond.* **4**, 239 (1960).
- [38] M.K. Rabinal, K.S. Sangunni, E.S.R. Gopal, *J. Non-Cryst. Solids* **188**, 98 (1995).
- [39] E.R. Shaaban, I.B.I. Tomsah, *J. Therm. Anal.* **105**, 191 (2011).
- [40] M. Lasocka, *Mater. Sci. Eng.* **23**, 173 (1976).
- [41] H.E. Kissinger, *Anal. Chem.* **29**, 1702 (1957).
- [42] J. Vazquez, P.L. Lopez-Aleman, P. Villares, R. Jimenez-Garay, *J. Alloys Comp.* **354**, 153 (2003).
- [43] W.H. Zachariasen, *J. Am. Chem. Soc.* **54**, 3841 (1932).
- [44] A.F. Loffe, A.R. Regel, *Prog. Semicond.* **4**, 239 (1960).
- [45] V. Sadgopam, H.C. Gotos, *Solid State Electron.* **8**, 529 (1965).
- [46] E. Mytilineou, *J. Opto. Adv. Mater.* **4**, 705 (2002).
- [47] Y. Kawamoto, S. Tsuchihashi, *J. Cream Assoc. Japan* **77**, 12 (1969).
- [48] A.H. Moharram, A.A. Abu-Sehly, M. Abu El-Oyoun, A.S. Soltan, *Physica B* **324**, 344 (2002).